Nano Energy 34 (2017) 556–561

Contents lists available at ScienceDirect

Nano Energy

journal homepage: www.elsevier.com/locate/nanoen

Communication

A novel wide bandgap conjugated polymer (2.0 eV) based on bithiazole for high efficiency polymer solar cells

Bing Guo[a], Wanbin Li[a], Xia Guo[a], Xiangyi Meng[b], Wei Ma[b], Maojie Zhang[a,*], Yongfang Li[a,c]

[a] Laboratory of Advanced Optoelectronic Materials, College of Chemistry, Chemical Engineering and Materials Science, Soochow University, Suzhou 215123, China

[b] State Key Laboratory for Mechanical Behavior of Materials, Xi'an Jiaotong University, Xi'an 710049, China

[c] Beijing National Laboratory for Molecular Sciences, CAS Key Laboratory of Organic Solids, Institute of Chemistry, Chinese Academy of Sciences, Beijing 100190, China

ARTICLE INFO

Keywords:
Wide bandgap
Conjugated polymer
Bithiazole
Polymer solar cells

ABSTRACT

An efficient wide bandgap conjugated polymer (PTZ6) based on alkoxylphenyl substituted benzodithiophene as donor unit and bithiazole as acceptor unit was developed for polymer solar cells (PSCs). The polymer exhibited a wide bandgap of 2.0 eV with strong absorption in the range of 300–620 nm, and a low-lying highest occupied molecular orbital (HOMO) energy level of −5.36 eV. The PSCs based on PTZ6: $PC_{71}BM$ show a PCE of 8.1% with a V_{oc} of 0.96 V, a J_{sc} of 10.9 mA cm^{-2} and a high FF of 76.7%, which is among the highest values for the fullerene PSCs based on conjugated polymer donors with bandgap near to 2.0 eV. Moreover, for this blend system, the photovoltaic performance of the devices changes little when the active layer thickness increases from 90 nm to 220 nm. More importantly, the non-fullerene PSCs based on PTZ6: ITIC exhibit a PCE of 10.3% with a high V_{oc} of 1.01 V, which should be the best value for the non-fullerene PSCs with the E_{loss} less than 0.6 eV to date. Our results indicate that PTZ6 is a promising wide bandgap polymer donor for the photovoltaic application in PSCs.

1. Introduction

Organic photovoltaics (OPVs), emerging as an environment friendly technology with function of converting solar energy into electricity, have attracted much attention due to their advantages of low cost, light weight, easy fabrication and potentials for making large area and flexible photovoltaic modules through roll-to-roll processing [1]. Generally, high-performance polymer solar cells (PSCs) based on bulk heterojunctions (BHJs) consist of a *p*-type conjugated polymer as donor and an *n*-type material (fullerene derivatives or *n*-type organic semiconductors (n-OSs)) as acceptor [2–4]. So far, significant progresses have been achieved in this filed with the power conversion efficiencies (PCEs) over 10% for single junction [5–7] and 11% for tandem solar cells [8,9].

In recent years, great efforts have been devoted to developing narrow bandgap (NBG) polymers [10–12] for the purpose of enlarging incident light harvesting and originally promoting short circuit current density (J_{sc}). Since it is very challenging to address the J_{sc}/open circuit voltage (V_{oc}) trade-off problem for NBG polymers in single junction PSCs [13], which will increase the intrinsic energy loss and limit the use of full solar spectrum, tandem devices by stacking two cells with BHJ active layers having complementary absorption spectra have been considered as a promising way to further enhance the performance of PSCs [14]. However, compared to the considerable efforts on developing outstanding NBG polymers, the exploration of novel wide bandgap (WBG) polymers with highly efficient performance have lagged behind, especially for polymers with bandgap near to 2.0 eV [15–18]. In addition, recently, non-fullerene *n*-OS acceptors are emerging as an attractive alternative because of their low production costs, easily tunable energy levels, excellent optical absorption properties, and good solubility in comparison with fullerene derivatives counterparts [4,19]. Encouraged by these advantages, a variety of donor-acceptor (D-A) structured non-fullerene *n*-OS acceptors were specially designed and synthesized, with the electron-deficient groups such as indanedione [20], benzothiadiazole [21,22], diketopyrolopyrrole [23,24], and rylene dimid [25–29] etc. PCEs near to 10% in non-fullerene PSCs have been reported by several groups [7,30–32], which are comparable to that of fullerene-based PSCs. It is well recognized that the complementary absorption spectra from the D-A pair is very important for highly efficient non-fullerene PSCs [33,34]. Since many excellent fullerene-free acceptors [35–37] exhibit strong absorption in the 600–800 nm region, the WBG polymers as donor materials will facilitate the use of

* Corresponding author.
E-mail addresses: guoxia@suda.edu.cn (X. Guo), mjzhang@suda.edu.cn (M. Zhang).

http://dx.doi.org/10.1016/j.nanoen.2017.03.013
Received 23 January 2017; Received in revised form 5 March 2017; Accepted 6 March 2017
Available online 07 March 2017

full solar spectrum and thus enhances the J_{sc} of solar cells. Moreover, the electronic energy levels of WBG polymers can appropriately match non-fullerene acceptors, which can reduce the energy loss and thus maximize the V_{oc} of the devices [7]. Therefore, it is urgent and desirable to design and synthesize superior WBG polymers for applications in the high-performance PSCs.

Among various acceptor units used in D-A copolymer photovoltaic materials, the electron-deficient bithiazole (BTz) unit has attracted much interest in the construction of WBG conjugated polymers for applications in PSCs because of its weak electron withdrawing ability, simple and planar structure [38–40]. Plenty of D-A copolymers based on BTz as acceptor unit have been reported, showing broad bandgap of ~1.9 eV [41–46] and PCEs over 6% [47]. For example, the polymer PBDTBTz-T based on bithiazole and benzodithiphene (BDT) with thiophene conjugated side chins (BDT-T) reported by our group, exhibited a bandgap of 1.89 eV and PCE of 6.09% [47]. Moreover, for the two-dimension (2D)-polymer donor materials based on BDT with conjugated side chains, the absorption spectra and molecular energy levels can be finely modulated by choosing suitable conjugated side chains [48,49]. For example, in previous work, we have shown that attaching meta-alkoxy-phenyl side chains to the BDT unit can make the absorption spectra blue-shifted to some extent and the highest occupied molecular orbital (HOMO) energy level effectively down-shifted in comparison with its counterparts with thiophene side chains [50,51]. More importantly, the PCEs of the corresponding PSCs also exhibited a great improvement despite of the broader bandgap.

Hence, in this work, we designed and synthesized a new WBG polymer, PTZ6, based on alkoxylphenyl substituted benzodithiophene as donor unit and bithiazole as acceptor unit as shown in Fig. 1a. The optical, electrochemical, photovoltaic properties and the morphology of the blend films were investigated. The polymer exhibits a strong absorption in the range of 300–620 nm, a low-lying HOMO energy level of −5.36 eV and a hole mobility of 1.29×10^{-3} cm^2 V^{-1} s^{-1}. The PSCs based on the blend of [6,6]-phenyl-C_{71}-butyric acid methyl ester ($PC_{71}BM$, Fig. 1a) and PTZ6 exhibit a high PCE up to 8.1% with a V_{oc} of 0.96 V, a J_{sc} of 10.9 mA cm^{-2} and a high fill factor (FF) of 76.7%, which is one of the highest values reported in the literature to date for fullerene PSCs based on conjugated polymers with bandgap near to 2.0 eV. Furthermore, the photovoltaic performance of PTZ6: $PC_{71}BM$-based PSCs is insensitive to variations of active layer thickness in the range of 90–220 nm. Considering that the absorption onset of PTZ6 is at 620 nm, we further fabricated non-fullerene PSCs using 3,9-bis (2-methylene-(3-(1,1-dicyanomethylene)-indanone))-5,5,11,11-tetrakis (4-hexylphenyl) -dithieno[2,3-d:2′,3′-d′]-s-indaceno[1,2-b:5,6-b′]dithiophene [35] (ITIC, Fig. 1a) as the electron acceptor. A high PCE of 10.3% with a J_{sc} of 14.1 mA cm^{-2} and a high V_{oc} of 1.01 V was achieved for the non-fullerene PSCs based on PTZ6: ITIC blend. These results indicate that PTZ6 is a promising polymer donor for the photovoltaic application in PSCs.

2. Results and discussion

2.1. Material synthesis and characterization

The synthetic route of PTZ6 is shown in Scheme S1 in Supporting Information. Compound 3 and 4 were synthesized according to our previously reported procedure [43–45,50]. PTZ6 was synthesized via a typical Stille-coupling reaction using toluene as solvent and $Pd(PPh_3)_4$ as catalyst. The polymer exhibits good solubility in common solvents, such as chloroform (CF), chlorobenzene (CB), and *o*-dichlorobenzene (*o*-DCB), thus offering good solution-processing condition for a high quality blend film. The number-average molecular weight (M_n) of PTZ6 is 31.3 kDa with a polydispersity index (PDI) of 1.88, evaluated by high temperature gel permeation chromatography at 160 °C using 1, 2, 4-trichlorobenzene as the eluent. The decomposition temperature (5% weight loss) was over 450 °C under inert atmosphere, as measured by thermogravimetric analysis (TGA, Fig. S1).

The absorption spectra of PTZ6 in solution and thin film are shown in Fig. 1b. The maximum absorption peak of PTZ6 is located at 522 nm in solution, while the peak is at 526 nm in thin film with a slight redshift. In addition, an enhanced absorption shoulder peak at 570 nm in thin film can be observed, which indicates the intermolecular π-π stacking interaction of the polymer. The absorption edge (λ_{onset}) is located at 620 nm, corresponding to an optical bandgap (E_g^{opt}) of 2.0 eV. Electrochemical cyclic voltammetry (CV) was performed to evaluate the electronic energy levels of the polymer (Fig. S2). The HOMO energy level (E_{HOMO}) of PTZ6 calculated from the onset of oxidation is −5.36 eV, which down-shifts by 0.15 eV compared with that of PBDTBTz-T (−5.21 eV) [44]. The lowest unoccupied molecular orbital (LUMO) energy level (E_{LUMO}) is −3.36 eV, which was deduced from the HOMO level and optical bandgap. The low-lying HOMO energy level of a polymer donor is beneficial for a high V_{oc} in PSCs. In

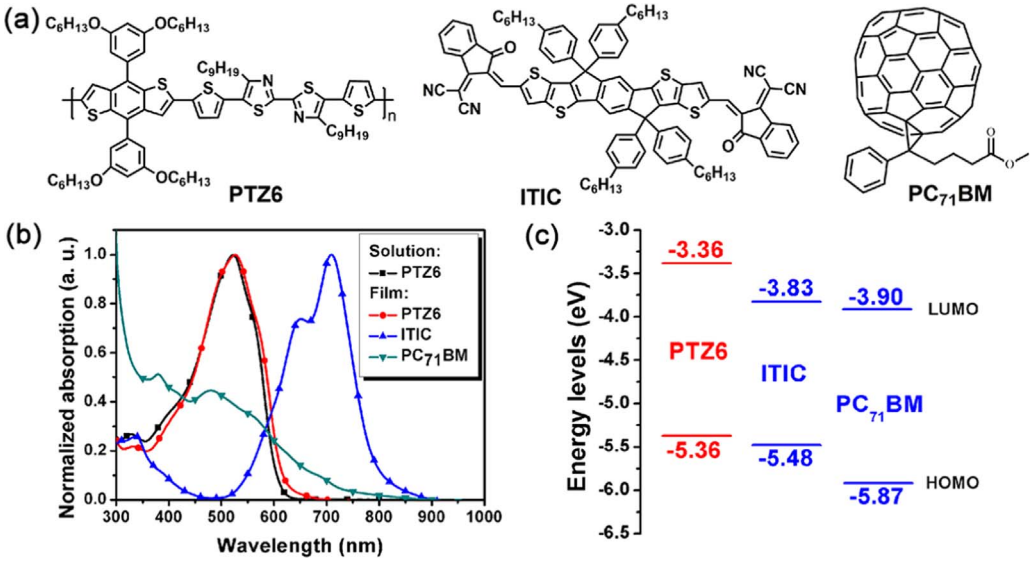

Fig. 1. (a) Chemical structures of PTZ6, ITIC and $PC_{71}BM$. (b) Absorption spectra of PTZ6 in chloroform and PTZ6, ITIC, and $PC_{71}BM$ in thin film. (c) Energy level diagram for the donor material and acceptors.

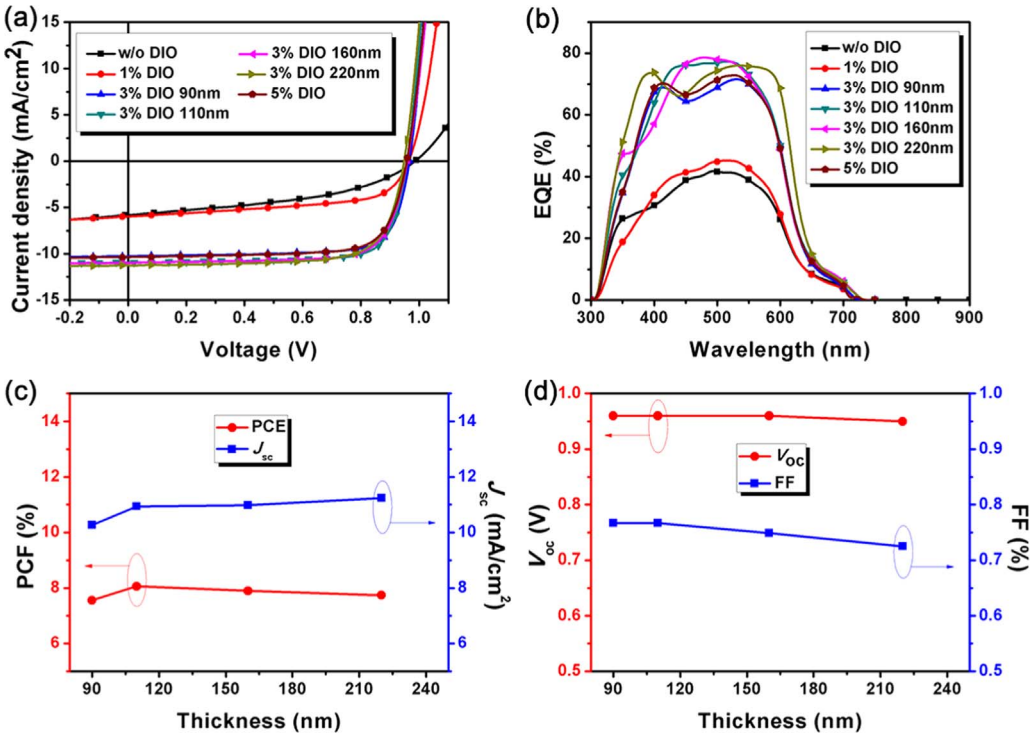

Fig. 2. (a) *J-V* characteristics and (b) EQE curves of solar cells based on PTZ6: $PC_{71}BM$ (1:1, w/w) with different processing conditions. (c) and (d) Photovoltaic parameters (PCE, J_{sc}, V_{oc} and FF) versus active layer thickness of PTZ6: $PC_{71}BM$ solar cells.

addition, the hole mobility of PTZ6 was measured by the space-charge-limited-current (SCLC) method (Fig. S8a and Table S3) and a value of 1.29×10^{-3} cm^2 V^{-1} s^{-1} was achieved.

2.2. Characterization of photovoltaic performance

The PSC devices were fabricated with an inverted structure of ITO (Indium tin oxide)/ZnO/Active layer/MoO_3/Al. The photovoltaic performance of PTZ6: $PC_{71}BM$-based PSCs were firstly investigated by the conventional procedure. The optimized D: A weight ratio is 1:1 (w/w), and a PCE of 2.52% is obtained with a high V_{oc} of 0.99 V (Fig. S3 and Table S1). To further improve the photovoltaic performance of the device, a small amount of 1,8-diiodooctane (DIO) was added to the solutions before the spin-coating process. Surprisingly, we found that DIO additive led to a significant improvement in device performance. The current density-voltage (*J-V*) characteristics and external quantum efficiency (EQE) curves are shown in Fig. 2 and the corresponding photovoltaic parameters are summarized in Table 1. Compared to the control device, the performance of the devices processed with 1% DIO showed a moderate improvement. Surprisingly, the PTZ6: $PC_{71}BM$-based device with 3% DIO additive yielded a high PCE of 8.1%, with enhanced J_{sc} of 10.9 mA cm^{-2} and high FF of 76.7%, despite slightly lower V_{oc}, which is one of the highest values reported in the literature to date for fullerene PSCs based on conjugated polymer donors with bandgap near to 2.0 eV. As shown in Fig. 2b, EQE was significantly enhanced for solar cells processed with 3% DIO as the solvent additive. The quantum efficiency values higher than 70% were observed at 420–560 nm; a maximum EQE of 77% at 510 nm was recorded, indicating efficient photon harvesting and charge collection within the device.

Table 1
Photovoltaic performance of solar cells based on PTZ6: $PC_{71}BM$ (1:1, w/w) with different processing conditions under the illumination of AM 1.5 G, 100 mW cm^{-2}.

DIO (v/v,%)	Thickness (nm)	V_{oc} (V)	J_{sc}[a] (mA cm^{-2})	FF (%)	PCE[b] (%)
w/o	85	0.99	5.8 (5.6)	43.7	2.5 (2.4)
1	100	0.96	6.0 (5.9)	58.0	3.3 (3.2)
3	90	0.96	10.3 (9.8)	76.7	7.6 (7.4)
3	110	0.96	10.9 (10.5)	76.7	8.1 (7.9)
3	160	0.96	11.0 (10.4)	74.9	7.9 (7.8)
3	220	0.95	11.2 (11.2)	72.5	7.7 (7.5)
5	100	0.96	10.4 (9.9)	74.6	7.4 (7.3)

[a] Values calculated from EQE in brackets.
[b] Average PCEs in brackets for 30 devices.

Furthermore, the dependency between the thickness of the active layers and the photovoltaic performance was also investigated based on the D: A weight ratio of 1:1 (w/w) with 3% DIO as additive. As shown in Fig. 2c-d and Table 1, when the active layer thickness increased from 90 nm to 220 nm gradually, the FF values of the devices dropped slightly from 76.7% for the PSC with the thickness of 90 nm to 72.5% for the PSC with the thickness of 220 nm, while the V_{oc} (ca. 0.96 ± 0.01 V) and J_{sc} (ca. 10.9 ± 0.5 mA cm^{-2}) were minimally changed. Therefore, the PSCs exhibited superior PCEs of 7.8 ± 0.3% when the thickness of the active layer changed from 90 nm to 220 nm. Interestingly, the FF values still remained higher than 72% when the thickness varied from 90 nm to 220 nm, probably resulted from the balanced charge transport and limited bimolecular recombination even in very thick active layers. On the basis of the above results, it can be concluded that the photovoltaic performance of the PSCs based on PTZ6: $PC_{71}BM$ is not sensitive to the variation of active layer thickness in the range of 90–220 nm.

Although high PCE over 8% has been achieved for PTZ6: $PC_{71}BM$-based PSCs, the active layers exhibit narrow photovoltaic response in the visible light range, which limits the J_{sc} and even PCE. Recently, ITIC [35] as a non-fullerene acceptor has attracted much attention due to its suitable energy levels, high electron mobility, and strong absorption from 600 to 780 nm region, which will well match the absorption spectra of PTZ6 and harvest more sunlight. As shown in Fig. 1b, the absorption spectra of PTZ6 film mainly overlaps that of the $PC_{71}BM$ spectrum in the 300–620 nm range but is complementary with that of ITIC. The blend film of PTZ6: ITIC (1:1, w/w) shows a wide absorption range from 300 to 780 nm (Fig. S4), which will contribute to a relatively high current density. As shown in the Fig. 1c, the LUMO

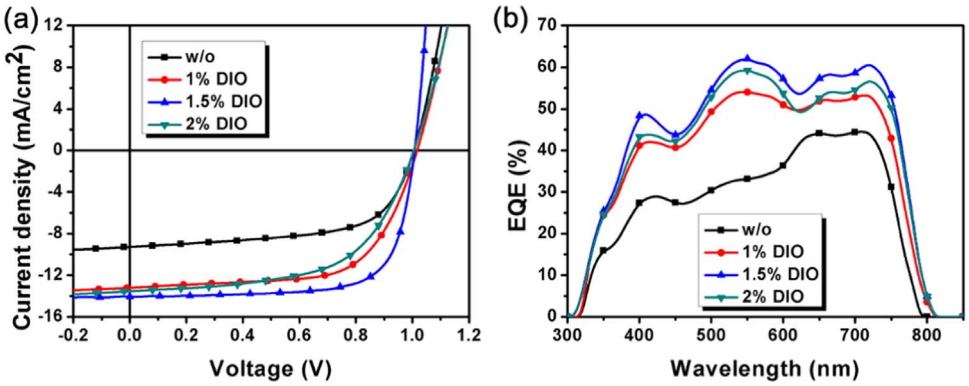

Fig. 3. (a) *J-V* characteristics and (b) EQE curves of solar cells based on PTZ6: ITIC (1:1, w/w) with different DIO additive contents.

energy levels offset ($\triangle E_{LUMO}$) between PTZ6 and ITIC (−3.83 eV) is larger than the empirical threshold of 0.3 eV for effective exciton dissociation, while it is also smaller than that between PTZ6 and $PC_{71}BM$, which is beneficial for a higher V_{oc} in the PSCs.

Accordingly, the non-fullerene PSCs based on PTZ6: ITIC blend with the same structure used in the $PC_{71}BM$-based PSCs were fabricated. The D/A weight ratios (PTZ6/ITIC, w/w) of the blend in the active layer were optimized (Fig. S5 and Table S2). The optimal D: A weight ratio is 1:1 (w/w), and a high V_{oc} of 1.01 V, a J_{sc} of 9.3 mA cm^{-2}, a FF of 62.1%, and a PCE of 5.8% were achieved. On the basis of the 1:1 (w/w) blend ratio, DIO was used to further improve the photovoltaic performance. The *J-V* characteristics and EQE curves are shown in Fig. 3 and the corresponding photovoltaic parameters are summarized in Table 2. Compared with the devices that were processed without any additive, the devices processed with DIO solvent additive exhibited higher J_{sc} and FF as well as similar V_{oc}; thus, PCE was enhanced. The best performance was obtained when 1.5% DIO was used, and the champion device yielded a high PCE of 10.3%, with a high V_{oc} of 1.01 V, a J_{sc} of 14.1 mA cm^{-2}, and a FF of 72.3%. To the best of our knowledge, this V_{oc} is among the top values for the ITIC-based non-fullerene PSCs. However, when the DIO content increased to 2%, both J_{sc} and FF were decreased, resulting in a relatively low PCE. As shown in Fig. 3b, EQE was obviously enhanced for the solar cells that were processed with DIO as the additive. The EQE spectrum of the device processed with 1.5% DIO covers a wide wavelength range from 300 to 800 nm, with the maximum peak up to 62% at 550 nm. Notably, the EQE values for solar cells in the range of 650–800 nm, where the absorption of PTZ6 is negligible, are quite comparable to those in the absorption range of the donor polymer (300–620 nm), indicating that the photons absorbed by ITIC are converted to electrons efficiently. These results indicate that the 0.12 eV HOMO energy offset (as shown in Fig. 1c) between PTZ6 and ITIC is sufficient to ensure the efficient hole transfer from ITIC to the polymer. Photoluminescence (PL) quenching experiments were carried out to investigate the efficiency of exciton dissociation and charge transfer at the D-A interface. As shown in Fig. S6, the PL intensities of both PTZ6 and ITIC in blend films are significantly quenched, which further proves the efficient charge transfer between the ITIC acceptor and the polymer donor under such a small ΔE_{HOMO} of 0.12 eV.

Table 2
Photovoltaic performance of solar cells based on PTZ6: ITIC (1:1, w/w) with different DIO additive contents under the illumination of AM 1.5 G, 100 mW cm^{-2}.

DIO (v/v,%)	V_{oc} (V)	J_{sc}[a] (mA cm^{-2})	FF (%)	PCE[b] (%)	Thickness (nm)
w/o	1.01	9.3 (8.9)	62.1	5.8 (5.7)	85
1	1.02	13.2 (12.3)	67.2	9.1 (9.0)	102
1.5	1.01	14.1 (14.0)	72.3	10.3 (10.1)	95
2	1.01	13.5 (13.2)	61.1	8.4 (8.3)	98

[a] Values calculated from EQE in brackets.
[b] Average PCEs in brackets for 30 devices.

It is well-known that there is a trade-off between V_{oc} and J_{sc} for the PSCs, so it is challenging to simultaneously maximize both high V_{oc} and high J_{sc} for the same blend system. Hence, minimizing the energy loss (E_{loss}) will play a key role in achieving a higher PCE. The E_{loss} is defined by $E_{loss}=E_g-eV_{oc}$, where E_g is determined by the smaller value of donor or acceptor materials [52]. Accordingly, E_{loss} of the PTZ6: ITIC system was found to be ~0.58 eV, deduced from V_{oc} of the PTZ6: ITIC system (1.01 V) and the E_g of ITIC (~1.59 eV) [35]. This value is even smaller than 0.6 eV that has been referenced as the empirical limit for PSCs [53]. Furthermore, the PCE of the PSC based on PTZ6: ITIC is the highest value among non-fullerene PSCs with E_{loss} less than 0.6 eV to date.

2.3. Characterization of molecular packing and morphology in the blend

Grazing incidence X-ray diffraction (GIXD) measurements were used to investigate the effect of the additive on the molecular orientation and packing of the blend films. The in-plane and out-of-plane GIXD profiles of neat and blend films with or without DIO additive treatment are displayed in Fig. 4. For the neat PTZ6 film, the in-plane profile shows obvious (100) diffraction peak at 0.31 $Å^{-1}$ with a *d*-spacing of 20.3 Å, whereas the out-of-plane shows a sharp and intensive peak at 1.66 $Å^{-1}$, corresponding to the (010) π-π staking with a *d*-spacing of 3.78 Å, indicating that the neat polymer film exhibits a dominated face-on molecular orientation relative to the substrate. The lamellar (100) peak of ITIC is located at 0.48 $Å^{-1}$ with a *d*-spacing of 13.09 Å in the out-of-plane profile. In as-cast PTZ6: $PC_{71}BM$ blend film, the π-π staking of the polymer was almost completely disturbed. The broad peak at q ≈1.4 $Å^{-1}$ is attributed to $PC_{71}BM$ aggregation [50]. When blended with ITIC, the π-π stacking peak of the polymer became slightly weak, and the lamellar peak of ITIC was completely disrupted by mixing with polymer. When using DIO as additive, the blend film exhibited distinct diffraction peaks at 0.48 $Å^{-1}$, indicating that the molecular packing of ITIC was enhanced in the blend film with the DIO treatment. We also calculated the coherence length of π-π staking, which was calculated from the full width at half maximum (FWHM) of out-of-plane using Scherrer equation [54]. The coherence length of PTZ6 π-π staking is 3.53 and 4.78 nm for PTZ6: $PC_{71}BM$ blend without and with DIO additive treatment, and 3.38 and 6.25 nm for PTZ6: ITIC blend without and with DIO additive treatment, respectively. The improved π-π staking ordering will be favorable for charge transport and thus device performance. Compared to PTZ6: $PC_{71}BM$ blend film, the π-π staking in the out-of-plane direction of PTZ6: ITIC blend film processed with DIO is distinctly stronger than that in the in-plane direction, suggesting that molecules take predominantly face-on orientation relative to the substrate. Clearly, the addition of a small amount of DIO into the

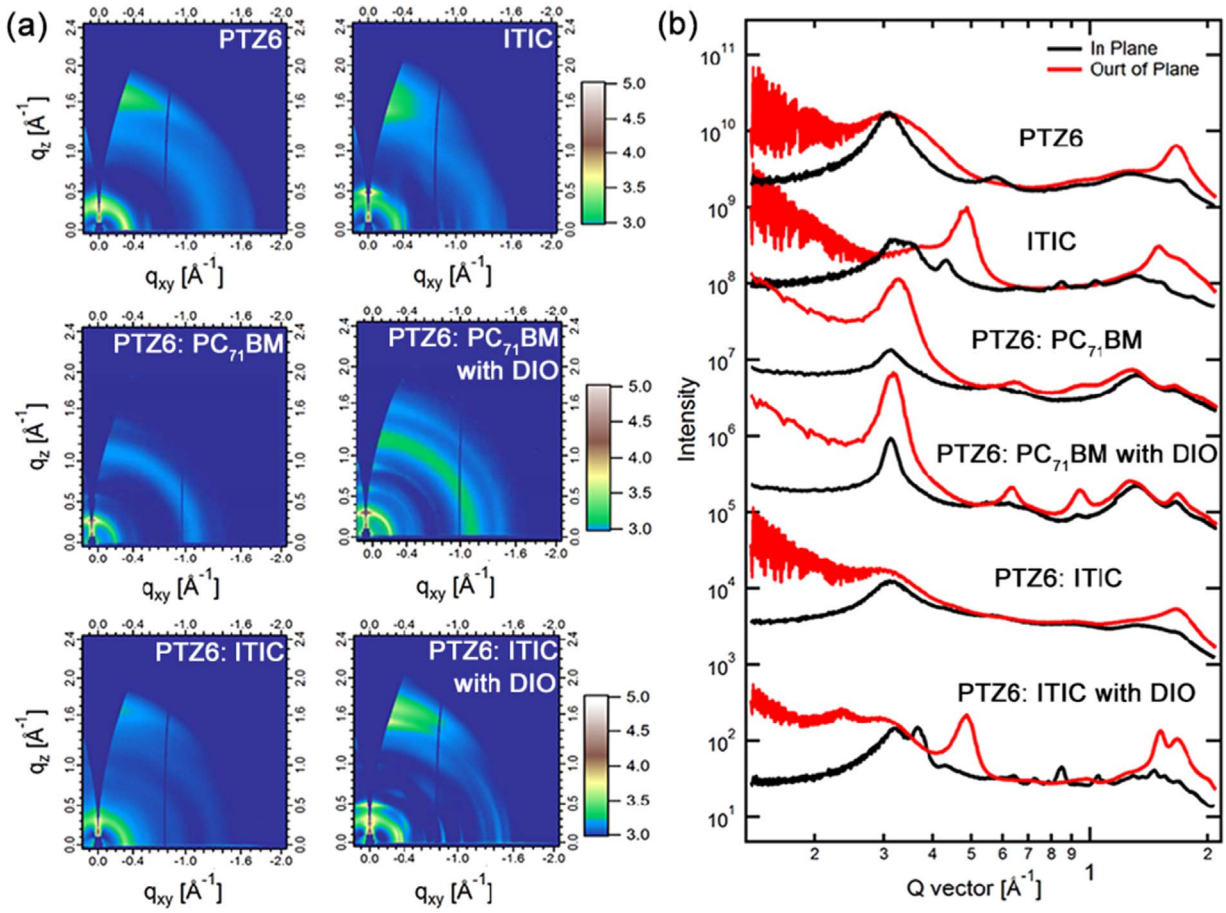

Fig. 4. (a) 2D GIXD patterns and (b) scattering profiles for pure PTZ6, ITIC and PTZ6: acceptor ($PC_{71}BM$ or ITIC) (1:1, w/w) blend films as-spun and processed with DIO (3% for PTZ6: $PC_{71}BM$, 1.5% for PTZ6: ITIC).

casting solutions promotes its high crystalline behavior of the blend film and strong face-on orientation, which are desirable to vertical charge transport thereby higher photovoltaic performance.

Furthermore, atomic force microscopy (AFM) and transmission electron microscopy (TEM) were also carried out to gain insight into the surface and bulk morphology of the active layers, respectively. As shown in Fig. S7, as-cast PTZ6: $PC_{71}BM$ film shows large domains with a root mean square (RMS) of 3.08 nm. When 3% DIO was added, smooth film is achieved with a RMS of 1.54 nm. In contrast to $PC_{71}BM$-based films, the addition of DIO in PTZ6: ITIC films leads to a higher RMS from 1.99nm to 7.90 nm. As shown in TEM images (Fig. 5), large PCBM domains are emerged in as-cast PTZ6: $PC_{71}BM$ film, while nanoscale fibrils can be obviously distinguished in film with 3% DIO additive. Interestingly, different from $PC_{71}BM$-based blend films, the as-cast PTZ6: ITIC blend film shows homogeneous morphology, and no distinct phase separation can be observed. When 1.5% DIO additive was added, obvious nanoscale phase separation can be observed in PTZ6: ITIC blend film. As the DIO content increased to 2%, the blend film showed large scale phase separation as shown in Fig. S8, which may cause more geminate recombination and bimolecular recombination and thus limits J_{sc} and FF of the device. When using DIO as additive, the opposite trend of the domains size in the blend film of polymer: fullerene and polymer: ITIC should be caused by the different of solubility of acceptors in the DIO or the different interaction with DIO, which has also been reported in other blend systems [55,56].

As mentioned above, it is clear that DIO additive has a positive effect for inducing the formation of good nanoscale structures, which promotes efficient exciton dissociation and charge transport [57]. In addition, PTZ6: $PC_{71}BM$ or ITIC blend films processed with DIO additive show higher and more balanced charge transport (hole mobility:

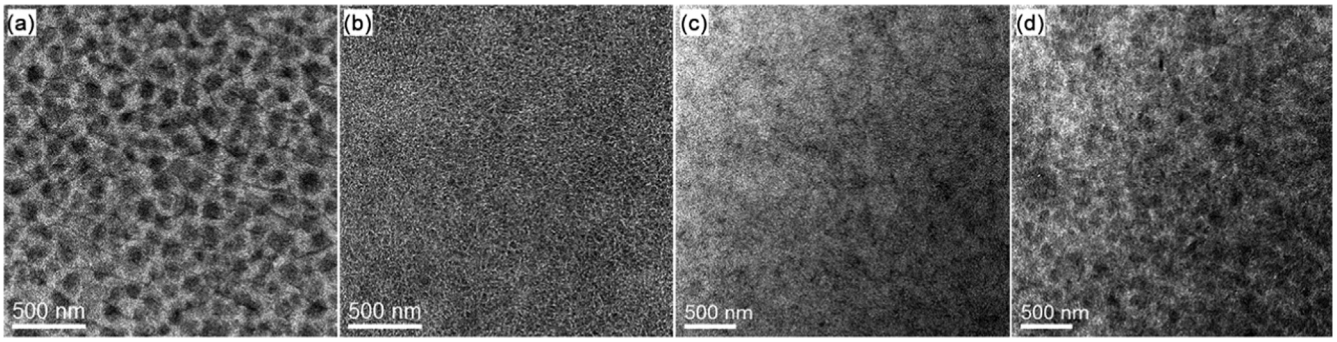

Fig. 5. TEM images of PTZ6: $PC_{71}BM$ (1:1, w/w) blend films: (a) without DIO; (b) with 3% DIO, and PTZ6: ITIC (1:1, w/w) blend films: (c) without DIO; (d) with 1.5% DIO.

1.13×10^{-3} cm^2 V^{-1} s^{-1}, electron mobility: 7.25×10^{-4} cm^2 V^{-1} s^{-1} for $PC_{71}BM$-based devices; hole mobility: 3.73×10^{-4} cm^2 V^{-1} s^{-1}, electron mobility: 2.16×10^{-4} cm^2 V^{-1} s^{-1} for ITIC-based devices) (Fig. S9 and Table S3). These results are attributed to better morphology with nanoscale bicontinuous phase separation, better molecular packing and strong face-on orientation in the blend films, which are consistent with GIXD, AFM and TEM analyses.

3. Conclusion

In summary, a new conjugated D-A copolymer PTZ6 based on alkoxylphenyl substituted benzodithiophene as donor unit and bithiazole as acceptor unit was designed and synthesized for photovoltaic applications. The polymer exhibited a wide bandgap of 2.0 eV and a low-lying HOMO energy level of −5.36 eV. The PSCs based on PTZ6: $PC_{71}BM$ show a PCE of 8.1% with a V_{oc} of 0.96 V, a J_{sc} of 10.9 mA cm^{-2} and a high FF of 76.7%, which is among the highest values for the fullerene PSCs based on the donor polymers with bandgap near to 2.0 eV. Moreover, for this blend system, the photovoltaic performance of the devices changes little when the active layer thickness increases from 90 nm to 220 nm. More importantly, the PSCs based on PTZ6: ITIC exhibit a PCE of 10.3% with a high V_{oc} of 1.01 eV, which should be the best value for the non-fullerene PSCs with the E_{loss} less than 0.6 eV to date. Our results indicate that PTZ6 is a promising WBG material for the photovoltaic application.

Acknowledgements

B. G. and W. L. contributed equally to this work. This work was supported by National Natural Science Foundation of China (NSFC) (No. 51422306, 51503135, 51573120, 91333204, 21504066 and 21534003), the Priority Academic Program Development of Jiangsu Higher Education Institutions, Jiangsu Provincial Natural Science Foundation (Grant No. BK20150332), Natural Science Foundation of the Jiangsu Higher Education Institutions of China (Grant No. 15KJB430027) and the Ministry of Science and Technology of China (No. 2014CB643501, 2016YFA0200700). X-ray data was acquired at beamlines 7.3.3 at the Advanced Light Source, which is supported by the Director, Office of Science, Office of Basic Energy Sciences, of the U.S. Department of Energy under Contract No. DE-AC02-05CH11231. The authors thank Dr. Chenhui Zhu at beamline 7.3.3 for assistance with data acquisition.

Appendix A. Supporting information

Supplementary data associated with this article can be found in the online version at doi:10.1016/j.nanoen.2017.03.013.

References

[1] G. Yu, J. Gao, J.C. Hummelen, F. Wudl, A.J. Heeger, Science 270 (1995) 1789.
[2] C.J. Brabec, N.S. Sariciftci, J.C. Hummelen, Adv. Funct. Mater. 11 (2001) 15.
[3] B.C. Thompson, J.M. Fréchet, Angew. Chem. Int. Ed. 47 (2008) 58.
[4] C.B. Nielsen, S. Holliday, H.-Y. Chen, S.J. Cryer, I. McCulloch, Acc. Chem. Res. 48 (2015) 2803.
[5] Z. He, B. Xiao, F. Liu, H. Wu, Y. Yang, S. Xiao, C. Wang, T.P. Russell, Y. Cao, Nat. Photon. 9 (2015) 174.
[6] Y. Liu, J. Zhao, Z. Li, C. Mu, W. Ma, H. Hu, K. Jiang, H. Lin, H. Ade, H. Yan, Nat. Commun. 5 (2014) 5293.
[7] W. Zhao, D. Qian, S. Zhang, S. Li, O. Inganäs, F. Gao, J.H. Hou, Adv. Mater. 28 (2016) 4734.
[8] H. Zhou, Y. Zhang, C.K. Mai, S.D. Collins, G.C. Bazan, T.Q. Nguyen, A.J. Heeger, Adv. Mater. 27 (2015) 1767.
[9] Z. Zheng, S. Zhang, J. Zhang, Y. Qin, W. Li, R. Yu, Z. Wei, J.H. Hou, Adv. Mater. 28 (2016) 5133.
[10] S.H. Liao, H.J. Jhuo, Y.S. Cheng, S.A. Chen, Adv. Mater. 25 (2013) 4766.
[11] W. Li, W.C. Roelofs, M.M. Wienk, R.A. Janssen, J. Am. Chem. Soc. 134 (2012) 13787.
[12] C. Liu, K. Wang, X. Gong, A.J. Heeger, Chem. Soc. Rev. 45 (2016) 4825.
[13] K. Kawashima, Y. Tamai, H. Ohkita, I. Osaka, K. Takimiya, Nat. Commun. 6 (2015) 10085.
[14] J.Y. Kim, K. Lee, N.E. Coates, D. Moses, T.-Q. Nguyen, M. Dante, A.J. Heeger, Science 317 (2007) 222.
[15] B. Guo, X. Guo, W.B. Li, X.Y. Meng, W. Ma, M.J. Zhang, Y.F. Li, J. Mater. Chem. A 4 (2016) 13251.
[16] Q. Liu, C. Li, E. Jin, Z. Lu, Y. Chen, F. Li, Z. Bo, ACS Appl. Mater. Interfaces 6 (2014) 1601.
[17] W. Gao, T. Liu, M. Hao, K. Wu, C. Zhang, Y. Sun, C. Yang, Chem. Sci. 7 (2016) 6167.
[18] S.C. Price, A.C. Stuart, L. Yang, H. Zhou, W. You, J. Am. Chem. Soc. 133 (2011) 4625.
[19] Y. Lin, X. Zhan, Mater. Horiz. 1 (2014) 470.
[20] K.N. Winzenberg, P. Kemppinen, F.H. Scholes, G.E. Collis, Y. Shu, T.B. Singh, A. Bilic, C.M. Forsyth, S.E. Watkins, Chem. Commun. 49 (2013) 6307.
[21] S. Holliday, R.S. Ashraf, C.B. Nielsen, M. Kirkus, J.A. Röhr, C.-H. Tan, E. Collado-Fregoso, A.-C. Knall, J.R. Durrant, J. Nelson, I. McCulloch, J. Am. Chem. Soc. 137 (2015) 898.
[22] J.T. Bloking, X. Han, A.T. Higgs, J.P. Kastrop, L. Pandey, J.E. Norton, C. Risko, C.E. Chen, J.-L. Brédas, M.D. McGehee, A. Sellinger, Chem. Mater. 23 (2011) 5484.
[23] S. Li, W. Liu, M. Shi, J. Mai, T.-K. Lau, J. Wan, X. Lu, C.-Z. Li, H. Chen, Energy Environ. Sci. 9 (2016) 604.
[24] J.W. Jung, W.H. Jo, Chem. Mater. 27 (2015) 6038.
[25] X. Zhang, Z. Lu, L. Ye, C. Zhan, J.H. Hou, S. Zhang, B. Jiang, Y. Zhao, J. Huang, S. Zhang, Y. Liu, Q. Shi, Y. Liu, J. Yao, Adv. Mater. 25 (2013) 5791.
[26] H. Li, T. Earmme, G. Ren, A. Saeki, S. Yoshikawa, N.M. Murari, S. Subramaniyan, M.J. Crane, S. Seki, S.A. Jenekhe, J. Am. Chem. Soc. 136 (2014) 14589.
[27] J. Lee, R. Singh, D.H. Sin, H.G. Kim, K.C. Song, K. Cho, Adv. Mater. 28 (2016) 69.
[28] A. Sharenko, C.M. Proctor, T.S. van der Poll, Z.B. Henson, T.Q. Nguyen, G.C. Bazan, Adv. Mater. 25 (2013) 4403.
[29] D. Meng, D. Sun, C. Zhong, T. Liu, B. Fan, L. Huo, Y. Li, W. Jiang, H. Choi, T. Kim, J.Y. Kim, Y. Sun, Z. Wang, A.J. Heeger, J. Am. Chem. Soc. 138 (2015) 375.
[30] H. Bin, Z. Zhang, L. Gao, S. Chen, L. Zhong, L. Xue, C. Yang, Y.F. Li, J. Am. Chem. Soc. 138 (2016) 4657.
[31] Y. Lin, F. Zhao, Q. He, L. Huo, Y. Wu, T.C. Parker, W. Ma, Y. Sun, C. Wang, D. Zhu, A.J. Heeger, S.R. Marder, X. Zhan, J. Am. Chem. Soc. 138 (2016) 4955.
[32] Y. Qin, M.A. Uddin, Y. Chen, B. Jang, K. Zhao, Z. Zheng, R. Yu, T.J. Shin, H.Y. Woo, J.H. Hou, Adv. Mater. 28 (2016) 9416.
[33] H. Lin, S. Chen, Z. Li, J.Y.L. Lai, G. Yang, T. McAfee, K. Jiang, Y. Li, Y. Liu, H. Hu, J. Zhao, W. Ma, H. Ade, H. Yan, Adv. Mater. 27 (2015) 7299.
[34] L. Gao, Z.G. Zhang, H. Bin, L. Xue, Y. Yang, C. Wang, F. Liu, T.P. Russell, Y.F. Li, Adv. Mater. 28 (2016) 8288.
[35] Y. Lin, J. Wang, Z.G. Zhang, H. Bai, Y.F. Li, D. Zhu, X. Zhan, Adv. Mater. 27 (2015) 1170.
[36] Y. Lin, Q. He, F. Zhao, L. Huo, J. Mai, X. Lu, C.-J. Su, T. Li, J. Wang, J. Zhu, Y. Sun, C. Wang, X. Zhan, J. Am. Chem. Soc. 138 (2016) 2973.
[37] S. Li, L. Ye, W. Zhao, S. Zhang, S. Mukherjee, H. Ade, J.H. Hou, Adv. Mater. 28 (2016) 9423.
[38] T. Yamamoto, H. Suganuma, T. Maruyama, T. Inoue, Y. Muramatsu, M. Arai, D. Komarudin, N. Ooba, S. Tomaru, S. Sasaki, K. Kubta, Chem. Mater. 9 (1997) 1217.
[39] Y. Lin, H. Fan, Y.F. Li, X. Zhan, Adv. Mater. 24 (2012) 3087.
[40] W.-Y. Wong, X.-Z. Wang, Z. He, K.-K. Chan, A.B. Djurišic, K.-Y. Cheung, C.-T. Yip, A.M.-C. Ng, Y.Y. Xi, C.S. Mak, W. Chan, J. Am. Chem. Soc. 129 (2007) 14372.
[41] M.J. Zhang, H. Fan, X. Guo, Y. He, Z. Zhang, J. Min, J. Zhang, G. Zhao, X. Zhan, Y.F. Li, Macromolecules 43 (2010) 5706.
[42] M.J. Zhang, H. Fan, X. Guo, Y. He, Z. Zhang, J. Min, J. Zhang, G. Zhao, X. Zhan, Y.F. Li, Macromolecules 43 (2010) 8714.
[43] M.J. Zhang, X. Guo, Y.F. Li, Macromolecules 44 (2011) 8798.
[44] M.J. Zhang, Y. Sun, X. Guo, C. Cui, Y. He, Y.F. Li, Macromolecules 44 (2011) 7625.
[45] M.J. Zhang, X. Guo, X. Wang, H. Wang, Y.F. Li, Chem. Mater. 23 (2011) 4264.
[46] X. Guo, M.J. Zhang, L. Huo, C. Cui, Y. Wu, J.H. Hou, Y.F. Li, Macromolecules 45 (2012) 6930.
[47] K. Wang, X. Guo, B. Guo, W.B. Li, M.J. Zhang, Y.F. Li, Macromol. Rapid Commun. 37 (2016) 1066.
[48] M.J. Zhang, X. Guo, S. Zhang, J.H. Hou, Adv. Mater. 26 (2014) 1118.
[49] C. Cui, W.-Y. Wong, Y.F. Li, Energy Environ. Sci. 7 (2014) 2276.
[50] M.J. Zhang, X. Guo, W. Ma, S. Zhang, L. Huo, H. Ade, J.H. Hou, Adv. Mater. 26 (2014) 2089.
[51] W. Li, B. Guo, C.M. Chang, X. Guo, M.J. Zhang, Y.F. Li, J. Mater. Chem. A 4 (2016) 10135.
[52] M.A. Faist, T. Kirchartz, W. Gong, R.S. Ashraf, I. McCulloch, J.C. de Mello, N.J. Ekins-Daukes, D.D. Bradley, J. Nelson, J. Am. Chem. Soc. 134 (2011) 685.
[53] D. Veldman, S.C. Meskers, R.A. Janssen, Adv. Funct. Mater. 19 (2009) 1939.
[54] S.J. Ko, W. Lee, H. Choi, B. Walker, S. Yum, S. Kim, T.J. Shin, H.Y. Woo, J.Y. Kim, Adv. Energy Mater. 5 (2015) 1401687.
[55] S.J. Lou, J.M. Szarko, T. Xu, L.P. Yu, T.J. Marks, L.X. Chen, J. Am. Chem. Soc. 133 (2011) 20661.
[56] J.K. Lee, W.L. Ma, C.J. Brabec, J. Yuen, J.S. Moon, J.Y. Kim, K. Lee, G.C. Bazan, A.J. Heeger, J. Am. Chem. Soc. 130 (2008) 3619.
[57] M.J. Zhang, X. Guo, W. Ma, H. Ade, J.H. Hou, Adv. Mater. 27 (2015) 4655.